Our NMR experiments confirm the above conclusion. After a sample is quenched the NMR frequencies show time dependencies divided into the same two domains. Moreover, as shown in Fig. 2, we observe strikingly different coexistence curves and critical isochores in our quenched and nonquenched experiments. In the nonquenched experiment long waiting times (over twelve hours) occur before any measurement is made near T_c. This insures that the xenon sample has come to equilibrium with the gravitational field. In the quenched experiment all measurements are made after a relatively short time, about 20–30 min following the quench. This time must be long enough to insure equilibrium between the liquid and vapor phases but short enough to insure minimal effects from gravitational gradients. As shown in Fig. 2 the quenching technique eliminates both the excess line broadening and the anomaly of two apparently separate signals (high-density gas near bottom of sample and low-density vapor near top of sample) which occurs well above T_c in our nonquenched experiments as a result of the warped (sigmoid) gravitational density profile.

We wish to acknowledge many helpful discussions with Joseph Sak concerning critical phenomena and with Gary S. Collins concerning computer programs. This work was supported in part by the National Science Foundation.

(a)Present address: Department of Physics, University of Utah, Salt Lake City, Utah 84112.

[1]S.-k. Ma, *Modern Theory of Critical Phenomena* (Benjamin, Reading, Mass., 1976), p. 352.

[2]J. M. H. Levelt Sengers, Physica (Utrecht) 73, 73 (1974).

[3]J. M. H. Levelt Sengers and J. V. Sengers, Phys. Rev. A 12, 2622 (1975).

[4]C. Domb, in *Phase Transitions and Critical Phenomena*, edited by C. Domb and M. S. Green (Academic, New York, 1974), Vol. 3, p. 357.

[5]G. A. Baker *et al.*, Phys. Rev. Lett. 36, 1351 (1976).

[6]J. C. Le Guillou and J. Zinn-Justin, Phys. Rev. Lett. 39, 95 (1977).

[7]E. Kanegsberg, B. Pass, and H. Y. Carr, Phys. Rev. Lett. 23, 572 (1969).

[8]L. R. Wilcox and D. Balzarini, J. Chem. Phys. 48, 753 (1968).

[9]L. M. Stacey, B. Pass, and H. Y. Carr, Phys. Rev. Lett. 23, 1424 (1969).

[10]D. Balzarini and K. Ohrn, Phys. Rev. Lett. 29, 840 (1972).

[11]W. T. Estler *et al.*, Phys. Rev. A 12, 2118 (1975).

[12]R. Hocken and M. R. Moldover, Phys. Rev. Lett. 37, 29 (1976).

[13]M. R. Moldover, private communication.

[14]F. J. Wegner, Phys. Rev. B 5, 4529 (1972); J. Camp *et al.*, Phys. Rev. B 14, 3990 (1976). A good example of this method of analysis is given by S. C. Greer, Phys. Rev. A 14, 1770 (1976).

[15]F. J. Wegner, in *Renormalization Group in Critical Phenomena and Quantum Field Theory: Proceedings of a Conference*, edited by J. D. Gunton and M. S. Green (Temple Univ. Press, Philadelphia, Pa., 1974); Joseph Sak and M. S. Green, private communication.

[16]J. Als-Nielsen and O. W. Dietrich, Phys. Rev. 153, 717 (1967).

[17]J. S. Kouvel and M. E. Fisher, Phys. Rev. 136, A1626 (1964).

Light Scattering from Bulk and Surface Spin Waves in EuO

P. Grünberg and F. Metawe

Institut für Festkörperforschung der Kernforschungsanlage Jülich, D-5170 Jülich, Federal Republic of Germany

(Received 22 August 1977)

We present results of light-scattering experiments on thermal acoustic spin waves in EuO. The Brillouin spectra show two peaks which can be shifted by an external magnetic field. One of these is identified as due to a modified bulk spin wave of the material. The other one, by its anomalous behavior on reversal of the magnetic field or change of the scattering geometry, reveals itself as a spin wave propagating along the surface of the crystal.

Recently it has been shown that light scattering from thermal acoustic magnons in suitable systems can yield extremely large cross sections.[1] It thus seems quite encouraging to apply this technique to the observation of surface magnons. This problem has recently been treated theoretically by Cottam.[2]

Up to now, surface spin waves have only been observed by microwaves[3] and their dispersion been tested up to wave vectors of a few hundred inverse centimeters. The wave vectors which can be investigated by inelastic scattering of visible light typically range between 10^5 and 10^6 cm^{-1}. Here we would like to report on a light-scattering experiment from the fcc ferromagnet EuO. In addition to the usual scattering from a bulk spin wave we observe scattering which is identified as due to a surface spin wave. To our knowledge this is the first time that there is clear experimental evidence for light scattering from surface spin waves.

The best candidates for the observation of surface spin waves in a light-scattering experiment, of course, are those systems where the scattering intensity is strong. It is the squares of the magneto-optic constants which determines the light-scattering intensity from spin waves.[4] The europium chalcogenides (EuX, with X=O, S, Se, or Te) are among the systems showing the strongest known magneto-optic effects.[5] At the same time, for EuO the penetration depth for green laser light (Ar^+, 5145 Å) is ~1200 Å, reducing to ~400 Å the depth which significantly contributes to the scattered light. This also favors the observation of scattering from surface spin waves because in cases of large penetration depth such scattering will be swamped by that from the bulk spin wave. Special care thus had to be taken with respect to the preparation of the surfaces. Best results were obtained by cleaving and subsequent thermal polishing. Good spectra can also be obtained from freshly cleaved surfaces although the amount of elastically scattered light is also quite high in this case.

The experiments were performed on a Tropel

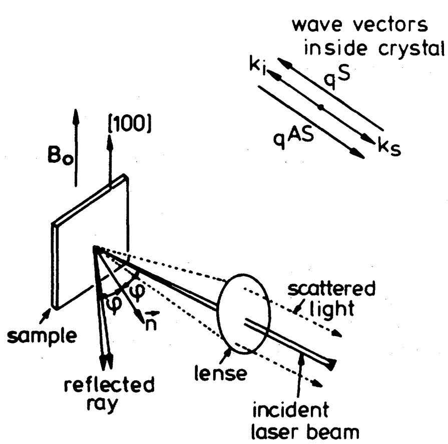

FIG. 1. Backscattering geometry. Because of refraction the wave vectors inside the crystal are somewhat inclined to the optical axis outside but in the plane of incident and reflected ray. The vector $\vec{n}$ denotes the normal on the sample plane.

three-pass Fabry-Perot interferometer. Depending on the frequency shift of the inelastic scattering, which in this case is a function of B_0, we chose free spectral ranges between 150 and 30 GHz. Also, in most cases, an observed frequency shift was measured with at least two different etalon distances. For cleaved surfaces a five-pass interferometer described elsewhere[6] had to be used. The scattering geometry is shown in Fig. 1. Here and in the following k_i and k_s are the wave vectors for incident and scattered light; q denotes the magnon wave vector where the superscripts S and AS stand for Stokes and anti-Stokes, respectively. Thin platelets parallel to the (100) planes were used. The magnetic field B_0 is parallel to a [100] direction lying in the sample plane and perpendicular to the plane defined by incident and reflected beams. Since the reflected laser beam must be kept out of the aperture of the instrument, the sample is tilted by an angle φ out of the direction perpendicular to the optical axis. The minimum value for φ amounts to approximately 5°. The Curie point of EuO is T_C = 69 K and so the samples had to be cooled. Magnetic fields were applied by a superconducting coil contained in the same cryostat. The analyzer direction for the polarization of the scattered light is always set perpendicular to the polarization of the incident light.

Typical spectra are shown in Fig. 2. There are two peaks, M_1 and M_2, which both sihft with changes of the magnetic field. Scattering from any kind of phonons, surface or bulk, can therefore be excluded. M_1 shows the usual Stokes–anti-Stokes anomaly typical for magnons.[4] The Stokes–anti-Stokes intensity ratio reverses on reversal of the polarization directions of incident and scattered light. It is not affected by a reversal of B_0. M_2, which is always observed at higher frequencies, also shows an anomaly but of different kind. First, we were never able to observe it as both Stokes *and* anti-Stokes at the same time. It comes either Stokes or anti-Stokes depending on the direction of B_0 or the way the sample is being tilted. There is no marked influence by the polarization directions as for M_1. The effect of changing the sense of the inclination of the sample is also shown in Fig. 2. For the wave-vector diagrams of Fig. 2 the experimental situation of Fig. 1 has to be viewed from above, parallel to the direction of B_0. If, for example, in one experiment M_2 is observed on the Stokes side then, on tilting the sample to the other side with respect to the optical axis, it comes anti-

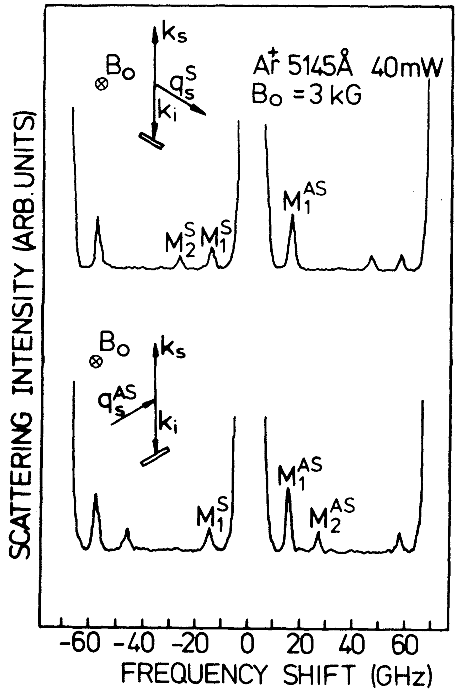

FIG. 2. Brillouin spectra from EuO at 45 K. The magnon wave vector q_s is constructed by considering the components of k_i and k_s to be parallel to the surface.

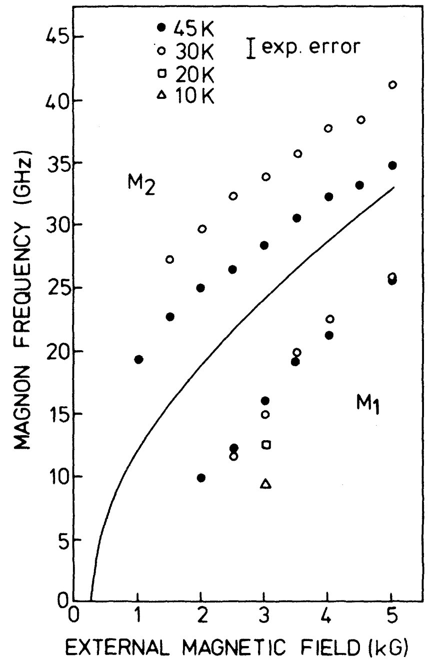

FIG. 3. Frequencies of peaks M_1 and M_2 of Fig. 2 as a function of external field at different temperatures. Solid line: bulk magnon from Eq. (1) where $B_{an} = +250$ G.

Stokes. The same happens when the sense of B_0 is reversed.

In the configuration used here the frequency of the normal or bulk spin waves is given by

$$\nu_m = (\gamma/2\pi)[(B_0 - B_{an} + Dq^2)(B_0 - B_{an} + Dq^2 + 4\pi M_s)]^{1/2}, \tag{1}$$

where $\gamma/2\pi = 0.28\times 10^7\ G^{-1}\ \sec^{-1}$. For the crystal anisotropy field we have at 45 K (30 K) $B_{an} = 100$ G (240 G) for the [100] direction.[7] The saturation magnetization $4\pi M_s$ has already reached its maximum value of 24 kG at $T=0$, within a few percent. For EuO the exchange term Dq^2 is of the order of 6 G and is neglected in the following. Figure 3 shows the experimental results. The points below the solid line, which displays ν_m from Eq. (1), correspond to M_1; the points above correspond to M_2. Because of its polarization-dependent Stokes–anti-Stokes anomaly, which is a general phenomenon,[4] we ascribe M_1 to a modified bulk magnon. It has to be regarded as modified because the frequencies deviate considerably from Eq. (1).

Since the scattered light is observed only from a 400-Å thin layer on the surface M_1, obviously is also influenced by the surface. The experimental points for M_1 taken at 45 and 30 K do not show any strong temperature dependence within experimental error. Additional measurements at 20 and 10 K with $B_0 = 3$ kG clearly show that M_1 shifts to lower frequencies when the temperature is decreased. This shift is too strong to be due to an increase of B_{an} in Eq. (1). We think that, again, this is due to an influence by the surface.

Most intriguing is the Stokes–anti-Stokes reversal of M_2 when B_0 is reversed or when the sample is tilted to the other side as is shown in Fig. 2. A rotation about 180° around the optical axis brings the experimental situation as shown in the upper part of Fig. 2 into the situation displayed in the lower part. A reversal of the magnetic field does the same, so that both operations are equivalent. In the pure backscattering configuration the optical axis is an axis of high symmetry. This is true in particular if the [100] axis of the crystal is parallel to B_0 as in the experiment described here. A rotation of 180° around this axis therefore leads to the same experimental situation regardless of the size of the angle φ. The backscattering configuration thus yields a contradiction with respect to the strange behavior of M_2. Let us assume therefore that M_2 stems from a spin wave which propagates along the surface of the crystal. This would reconcile the experimental findings with symmetry considerations. Because of the surface, the symmetry is just lowered in such a way that the equivalence of the Stokes and anti-Stokes wave vector is lifted. This can easily be seen by considering a right- (or left-) handed coordinate system where two axes are given by B_0 and a vector normal to the surface. Depending on whether B_0 is up or down, the third axis becomes identical with the Stokes *or* anti-Stokes wave vector. The existence of nonreciprocal modes in microwave guides[8] thus suggests that the M_2 peak is due to a surface wave which is only able to propagate in one direction given by the third axis but not in the opposite.

Another indication which points to a surface effect for M_2 is the fact that by an increase in the angle φ in Fig. 1 the ratio of the intensities of M_1 and M_2 changes in favor of M_2: The intensity of M_1 decreases quite considerably and that of M_2 increases. At small angles ($\varphi \approx 7°$) M_2 was not observable. At $\varphi = 65°$, M_2 is almost as strong as M_1 on the strong side. When the angle φ is changed, the measured frequencies stay constant within experimental error for both M_2 and M_1. Since different angles φ produce different wave-vector components of the incident and scattered light parallel to the surface, this means that there is no observable dispersion for the surface wave.

It might appear somewhat surprising that the surface wave has a higher frequency than that of the bulk. In other cases, as for phonons and plasmons, a lowering of the frequency is found. One should consider, however, that a surface spin wave sees the static magnetization of the bulk and an analog to this is absent for surface phonons and plasmons. In fact it has been shown[3] that in the magnetostatic limit the frequency of a surface spin wave in the present geometry is given by

$$\nu_s = (\gamma/2\pi)[B_0 + (4\pi M_s/2)]. \tag{2}$$

For EuO this yields a minimum frequency of $\nu_s = 34$ GHz for $B_0 = 0$, which is even higher than the observed low-field values of M_2. Hence, if at all, Eq. (2) is only applicable with modifications to the present case. These could, for example, lie in the presence of magnetic surface reconstruction which means that a different type of magnetic order can exist at the surface. An additional spin-wave branch going to finite frequencies as $q \to 0$ can appear.[9] It is unlikely that a light-scattering experiment is well suited to reveal deviations of the magnetic order in detail. We think, however, that at least we have an indication that the net in-plane magnetization close to the surface of the sample is reduced. Canting of the spins with respect to each other or jointly into the direction normal to the sample plane could be responsible for this. In this case the $4\pi M_s$ term in Eq. (1) is reduced, which could explain the frequency downshift for M_1. The canting then obviously becomes stronger at lower temperatures. From our experiments we have another indication that this happens. The above-described Stokes–anti-Stokes anomaly for M_1 is only possible if both longitudinal and transverse magneto-optic effects are present in the scattering mechanism.[4] For a spin wave propagating parallel to the magnetization, i.e., for the present case of magnetization normal to the surface, the scattering mechanism in the backscattering geometry is purely transverse and there should be no Stokes–anti-Stokes anomaly. This exactly what is observed for M_1 at low enough temperatures (10 K).

To conclude, there is experimental evidence that, in addition to a modified bulk spin wave, a surface spin wave has been observed in the (100) planes of EuO. Its frequency lies considerably above the frequencies of corresponding bulk spin waves. More detailed measurements are currently under way.

We should like to thank W. Zinn for stimulating discussions and interest in this work. We are indebted to K. Fischer for providing the single crystals. A great deal of support, which is gratefully acknowledged, has also been provided by J. R. Sandercock of RCA, Zürich, in the performance of the experiments which required a five-pass interferometer.

[1]J. R. Sandercock, Solid State Commun. 15, 1715 (1974).

[2]M. G. Cottam, J. Phys. C 9, 2137 (1976).

[3]A review has been given by T. Wolfram and R. E. Dewames, Prog. Surf. Sci. 2, Pt. 4 (1972).

[4]W. Wettling, M. G. Cottam, and J. R. Sandercock, J. Phys. C 8, 211 (1975).

[5]See, for example, J. Schoens, Z. Phys. B 20, 345 (1975).

[6]J. R. Sandercock, RCA Rev. 36, 89 (1975).

[7]R. S. Hughes, G. E. Everett, and A. W. Lawson, Phys. Rev. B 9, 2394 (1974).
[8]B. Lax and K. J. Button, *Microwave Ferrites and Ferrimagnetics* (McGraw-Hill, New York, 1962).
[9]C. Demangeat, D. L. Mills, and S. E. Trullinger, Phys. Rev. B 16, 522 (1977).

Electronic Structure of Semiconducting Films upon Ordering, as Observed by Double-Beam Photoemission

L. D. Laude, M. Lovato, M. C. Martin, and M. Wautelet
Université de l'Etat, B-7000 Mons, Belgium
(Received 27 June 1977)

The evolution of the electronic structure of disordered Te and Ge films upon thermal annealing and/or laser irradiation has been traced with use of the newly developed double-beam photoemission technique. In particular, it is shown that, contrary to what occurs in Te films, the onset of short-range crystalline ordering appears abruptly and uniformily within the Ge films, but over a much too short range to avoid $\vec{k}$ randomization before emission of the electrons.

The field of disordered solids is generally recognized as a puzzling one. However, among the positive information collected so far, atomic distribution studies have shown that crystalline short-range order is more or less present in disordered films. In parallel, photoemission has indicated that the structure of the crystalline valence-band density of states (DOS) would seem generally to be much less affected by the absence of long-range order in the disordered films than the conduction-band DOS.

Upon thermal annealing, as the atomic configuration evolves towards the crystal with increasing temperature, the electronic structure of the films, as seen by photoemission, resembles more and more that of the crystal. However, because of the limited resolution of photoemission, it was never possible to identify clearly any intermediate phase in that evolution. It was the purpose of the present work to investigate such ordering mechanisms developing in disordered semiconducting films (namely Ge and Te) upon thermal annealing and/or laser irradiation. It has been shown recently[1] that the possibility exists to modulate the photoemission current of a solid by using a flash-excited dye-laser (secondary) beam focused onto the sample together with the continuous uv (primary) beam. This double-beam photoemission technique (DBP) has proved to provide extremely precise information on the electronic structure of crystals.

Following arguments developed earlier,[1] DBP may be regarded as a two-step optical process via *real* intermediate conduction states. In the case of a crystal, the resulting DBP electron distributions can be expressed by

$$N(E, h\nu_{\text{uv}}, h\nu_L) = \sum_{\vec{k}} P(E,\vec{k})\,|\langle M_{VC_1}(\vec{k})\rangle|^2 \delta(E_V(\vec{k}) + h\nu_L - E_{C_1}(\vec{k}))$$
$$\times\big[\,|\langle M_{C_1C_3}(\vec{k})\rangle|^2 \delta(E_{C_1}(\vec{k}) + h\nu_{\text{uv}} - E_{C_3}(\vec{k}))\,\delta(E - E_{C_3}(\vec{k}))$$
$$+\,|\langle M_{VC_2}(\vec{k})\rangle|^2 \delta(E_V(\vec{k}) + h\nu_{\text{uv}} - E_{C_2}(\vec{k}))\,\delta(E - E_{C_2}(\vec{k}))\big], \tag{1}$$

where V and C label electron-state energy levels in the valence and conduction bands, respectively, $P(E,\vec{k})$ is the usual escape function of excited electrons, and M denotes the various matrix elements involved, with the summation running over the whole Brillouin zone.

The first term on the right-hand side of Eq. (1) describes the pulsed laser excitation of valence electrons into conduction states, followed by the uv excitation of these once-excited electrons into higher conduction states (process 1, in Ref. 1); the second term represents the uv excitation of valence electrons the density of which has been modulated through laser excitation (process 2, in Ref. 1).[2] In the absence of periodicity, $\vec{k}$ conservation does not hold and Eq. (1) may be reduced to two distributions